Available online at www.sciencedirect.com

ScienceDirect

Journal of the Chinese Medical Association 81 (2018) 912–919

www.jcma-online.com

Original Article

Can imaging distinguish between low-grade and dedifferentiated parosteal osteosarcoma?

Han-Ying Lin [a], Hung-Ta Hondar Wu [a,*], Po-Kuei Wu [b], Ching-Lan Wu [a], Paul Chih-Hsueh Chen [c], Wei-Ming Chen [b], Wan-Yuo Guo [a]

[a] *Department of Radiology, Taipei Veterans General Hospital, School of Medicine, National Yang-Ming University, Taipei, Taiwan, ROC*
[b] *Department of Orthopaedics, Taipei Veterans General Hospital, School of Medicine, National Yang-Ming University, Taipei, Taiwan, ROC*
[c] *Department of Pathology, Taipei Veterans General Hospital, School of Medicine, National Yang-Ming University, Taipei, Taiwan, ROC*

Received June 28, 2017; accepted January 15, 2018

Abstract

Background: Most instances of the parosteal osteosarcoma (OGS) are low-grade tumors. However, some parosteal OGSs undergo dedifferentiated transformation. Dedifferentiated parosteal OGS can cause distant metastasis and poor survival, and preoperative chemotherapy may be warranted. This study provides imaging clues for dedifferentiated parosteal OGS before treatment.
Methods: The study retrospectively enrolled 23 patients with histologically proven parosteal OGS, including 69.6% (n = 16) low-grade and 30.4% (n = 7) dedifferentiated types. Preoperative images including radiography and magnetic resonance imaging were reviewed. The following imaging parameters and clinical outcomes were evaluated: 1) average age; 2) sex; 3) tumor size; 4) presence of string sign; 5) necrosis; 6) hemorrhage; 7) solid soft tissue component; 8) perforating vessels; 9) ossification grade; 10) marginal ossification; 11) periosteal reaction; 12) sunburst reaction; 13) bone marrow edema; 14) bone marrow invasion; 15) perifocal soft tissue edema; 16) adjacent joint involvement; 17) adjacent neurovascular bundle compression; 18) regional lymph node; 19) bone metastasis; 20) preoperative lung metastasis; 21) follow-up lung metastasis; and 22) recurrence.
Results: The average maximal tumor sizes were 7.1 cm and 10.9 cm in low-grade and dedifferentiated types, respectively ($p = 0.033$). Sunburst periosteal reaction was visualized in two cases of low-grade type (12.5%) and four cases of the dedifferentiated type (57.1%) ($p = 0.025$) of parosteal OGS. None of our studied cases revealed preoperative lung metastasis. In the follow-up chest computed tomography, lung metastasis was noted in two cases of conventional type (14.2%), and four cases of dedifferentiated type (57.1%) ($p = 0.040$) of parosteal OGS. In receiver operating characteristic (ROC) curve analysis, the average tumor size and sunburst periosteal reaction showed good specificity (AUC = 0.070 and 0.072, respectively).
Conclusion: Compared with low-grade types, dedifferentiated parosteal OGS exhibits a considerably larger tumor size, more sunburst periosteal reaction, and a more frequent development of lung metastasis in the disease course. Tumor size and sunburst periosteal reaction are the most crucial imaging diagnostic factors.

Keywords: Bone tumor; Dedifferentiated parosteal osteosarcoma; MRI; Sunburst periosteal reaction

1. Introduction

Osteosarcoma (OGS) is the most common primary bone tumor in children and adolescents (4.4 cases per 1 million persons annually).[1–5] The World Health Organization currently classifies OGS into conventional, telangiectatic, small cell, low-grade central, secondary, periosteal, high-grade

Conflicts of interest: The authors declare that they have no conflicts of interest related to the subject matter or materials discussed in this article.

* Corresponding author. Dr. Hung-Ta Hondar Wu, Department of Radiology, Taipei Veterans General Hospital, 201, Section 2, Shi-Pai Road, Taipei 112, Taiwan, ROC.
E-mail address: hondar.wu@gmail.com (H.-T. Hondar Wu).

https://doi.org/10.1016/j.jcma.2018.01.014

surface, and parosteal types.[1,2] Parosteal OGS is rare, but is the most common juxtacortical OGS, accounting for approximately 4%−5% of all cases of OGS.[1,6,7] This condition occurs most commonly between the age of 10 and 39.[1] The tumor usually arises from the metaphysis of long bones, with the posterior aspect of the distal femur being the most common site (approximately 62%−70% of cases).[1,8] The typical radiological presentations of parosteal OGS are a lobulated, exophytic mass with central dense ossification adjacent to the bone, a cleavage plane separating the tumor and adjacent normal cortex (the so-called string sign), and the lack of an aggressive periosteal reaction.[1]

Most of the parosteal OGSs were low-grade tumors (Broder's Grade 1−2). Compared with the conventional OGS, low-grade parosteal OGS has a more favorable outcome. The 5-year survival rate was reported as 86−91%, and the distant metastasis rate was lower than 5%.[1,6] Due to advantageous clinical outcomes and histological patterns, neither neoadjuvant nor adjuvant chemotherapy were suggested.[9] However, approximately 24% of low-grade parosteal OGSs undergo dedifferentiation. Dedifferentiated parosteal OGS is a rare variation that is not yet well-recognized. Dedifferentiated parosteal OGS has only been described in case reports and small series.[6−8] Compared with low-grade parosteal OGS, dedifferentiated parosteal OGS possesses a higher capability of distant metastasis in association with a poor clinical outcome.

Histologically, dedifferentiated parosteal OGS is composed of two distinct components: high-grade (Broder's Grade 3−4) and low-grade components. The limited focal high-grade transformation makes dedifferentiated parosteal OGS difficult to correctly diagnose by preoperative biopsy.[9,10] This limitation leads pathologists and clinicians to make uncertain diagnoses or even administer erroneous treatments. Thus, the combined use of alternative methods such as imaging to maximize the precision of diagnoses is crucial. The purpose of this study was to assess the imaging characteristics of parosteal OGS, and compare the imaging presentations between low-grade and dedifferentiated parosteal OGS.

2. Methods

2.1. Patient selection

Between January 2004 and July 2016, patients with histologically proved parosteal OGS were retrospectively enrolled in this study. The tumor pathology of all the studied cases were proven by surgical wide excision or open biopsy, except one case in the low-grade parosteal OGS group, which was proven by computed tomography (CT)-guided biopsy, and was lost to follow-up in our hospital. One patient presented with an initial histological diagnosis of low-grade parosteal OGS in the first wide excision, but with local recurrence 1 year later and received a second operation with a histological diagnosis of transformed dedifferentiated parosteal OGS. This patient was placed in the dedifferentiated parosteal OGS group.

This study has been approved by the Institutional Review Board of Taipei Veterans General Hospital.

The study contained 23 cases in total (M/F = 9/14, onset age range between 13 and 46, average 23.1 years) including low-grade parosteal OGS (n = 16, 69.6%) and dedifferentiated parosteal OGS (n = 7, 30.4%).

2.2. Imaging modalities

The imaging modalities included radiography and magnetic resonance imaging (MRI) for tumor evaluation, and noncontrast CT of the chest for lung metastasis evaluation both preoperatively and in follow-up studies. All the image surveys were obtained 2 weeks before the biopsy or wide excision.

The MRI was performed using 1.5 T GE HDxt scanners to obtain the coronal T1-weighted imaging (WI) [repetition time (TR)/echo time (TE) = 525/5−28] and T2-WI (TR/TE = 5900/60), axial T1-WI (TR/TE = 600/5−28), and T2-WI (TR/TE = 5900/60), and sagittal scans (T2-WI) (TR/TE = 3375/60) in precontrast imaging. Subsequently, a post-Gadolinium contrast scan (Gadovist, 1 mmoL/mL) was performed to obtain the coronal or sagittal scans (T1-WI with fat saturation, TR/TE = 750/5−28) and axial scans (T1-WI with fat saturation). Matrix = 320x224, slice thickness = 4 mm, number of excitations (NEX) = 2, echo train length = 3−20, bandwidth = 16.67−62.25.

A chest CT was performed using an Aquilion 64 (Tokyo, Japan), with a noncontrast CT scan, scan range from the pulmonary apex to adrenal glands, slice thickness of 5 mm, tube voltage of 120 kVp, pitch of 1.484, and an effective mAs of 0.5*64 mAs.

2.3. Imaging analysis

We analyzed the following imaging parameters of parosteal OGS blindly and without knowing the histology type: 1) average age; 2) sex; 3) tumor size: maximal tumor dimension in either plane; 4) presence of the string sign: defined as a radiolucent cleavage plane on radiograph between portions of the tumor and cortex of the affected bone; 5) necrosis: tumor necrosis often at the central part with a low signal on T1-WI, and high signal on T2-WI; 6) hemorrhage: subacute hemorrhage with a high signal on T1-WI and high signal on T2-WI without fat saturation; 7) solid soft tissue component: solid component in the tumor part with postcontrast enhancement; 8) visualized perforating vessels with the tumor mass; 9) ossification grading in tumor: assigned according to the radiography, in which grade 0 denotes no ossification, grade 1 is less than a third ossification area, grade 2 is between one third and two thirds ossification area, and grade 3 is over two thirds ossification area to total ossification; 10) presence of marginal ossification: defined as bone formation at the periphery of the tumor; 11) presence of a periosteal reaction, which is a radiographic finding that occurs with periosteal irritation; 12) the presence of sunburst periosteal reaction, which is an aggressive form of periosteal reaction defined as an irregular linear radio-opacity perpendicular to the cortex; 13) the

presence of bone marrow edema, with hypointense signal in T1-WI and hyperintense signal in T2-WI observed in the bone marrow on MRI; 14) bone marrow invasion: with tumor invasion to bone marrow; 15) perifocal soft-tissue edema; 16) adjacent joint involvement by the tumor; 17) adjacent neurovascular bundle compression; 18) regional lymph node enlarged more than 1 cm in diameter; 19) the presence of neighboring bone metastasis (based on MRI); 20) the presence of preoperative lung metastasis (based on chest CT); 21) the presence of lung metastasis in the follow-up studies (based on chest CT); and 22) the presence of local recurrence.

Two radiologists who had specialized in musculoskeletal imaging (with 20 years of experience and 1 year of experience, respectively) examined and evaluated the imaging parameters and signs through consensus.

2.4. Statistical analysis

A statistical analysis with an independent Student's t test and chi squared test was used to determine the differences between the two groups. The numeric and continuous data such as patient's age and tumor size were analyzed with an independent Student's t test. The categorical data such as sex, ossification grade, periosteal reaction, and lung metastasis, were analyzed with a chi squared test. A receiver operating characteristic (ROC) curve analysis was performed to assess the diagnostic accuracy of the imaging parameters. All statistical analyses were performed using SPSS Statistics version 21.0. Results with p values lower than 0.05 were considered statistically significant.

3. Results

Among the 23 cases of parosteal OGS, 11 (47.8%) occurred in the distal femur, two (8.7%) in the proximal femur, four (17.4%) in the humerus, four (17.4%) in the tibia, one (4.3%) in the rib, and one (4.3%) in the vertebral body. The follow-up time for bone metastasis, lung metastasis, and recurrence ranged from 16 to 60 months (≦5 years), with an average time of 28.2 months. Two cases were not included in the follow-up analysis due to one having a follow-up time of less than 1 year, and one being lost to follow-up for 2 years. The results of the parameters in low-grade and dedifferentiated parosteal OGS types are summarized in Table 1.

The average age was 27.6 years and 23.6 years in the low-grade and dedifferentiated type, respectively ($p = 0.369$). The sex distribution indicated no significant difference between the two groups, with the ratio of males to females being 6:10 in the low-grade type and 3:4 in the dedifferentiated type, respectively ($p = 0.809$).

The maximal tumor size was in the range of 3.2 cm−17.7 cm, with an average size of 7.1 cm in the low-grade type, and 10.9 cm in dedifferentiated type. ($p = 0.033$).

Five patients in low-grade type exhibited string signs (31.3%), whereas three patients in dedifferentiated type were revealed to have string signs (42.9%), but there was no significant difference between the two groups ($p = 0.591$) (Fig. 1).

Periosteal reaction with either type was observed in 10 patients in the low-grade parosteal OGS group (62.5%), including five patients with Codman triangle, two patients with sunburst periosteal reaction, two patients with solid periosteal reaction,

Table 1
Comparison of the imaging findings of low-grade and dedifferentiated parosteal osteosarcoma.

Parameters	Total (n = 23)	Low grade type (n = 16)	Dedifferentiated (n = 7)	p
Age average	26.4	27.6	23.6	0.369
Sex (male: female)	9:14	6:10	3:4	0.809
Averaged tumor maximal length (cm)	8.2	7.1	10.9	0.033[a]
String sign	8 (34.8%)	5 (31.3%)	3 (42.9%)	0.591
Necrosis	11 (47.8%)	6 (37.5%)	5 (71.4%)	0.134
Hemorrhage	3 (13.0%)	2 (12.5%)	1 (14.3%)	0.907
Soft tissue component	21 (91.3%)	15 (93.7%)	6 (85.7%)	0.740
Perforating vessel	10 (43.5%)	7 (43.8%)	3 (42.9%)	0.968
Average ossification grade	2.6	2.5	2.7	0.619
Marginal ossification	8 (34.8%)	6 (37.5%)	2 (28.5%)	0.679
Periosteal reaction	16 (69.6%)	10 (62.5%)	6 (85.7%)	0.266
Periosteal reaction: sunburst	6 (26.1%)	2 (12.5%)	4 (57.1%)	0.025[a]
Bone marrow edema	16 (69.6%)	10 (62.5%)	6 (85.7%)	0.461
Bone marrow invasion	12 (52.2%)	6 (37.5%)	4 (57.1%)	0.332
Soft tissue edema	21 (91.3%)	14 (87.5%)	7 (100.0%)	0.544
Joint involvement	1 (4.3%)	1 (6.3%)	0 (0.0%)	0.499
Neurovascular bundle compression	15 (65.2%)	9 (56.3%)	6 (85.7%)	0.172
Lymph node involved	2 (8.7%)	2 (12.5%)	0 (0.0%)	0.328
Bone metastasis	0 (0%)	0 (0%)	0 (0%)	–
Pre-operative lung metastasis	0 (0%)	0 (0%)	0 (0%)	–
Follow-up lung metastasis	6 (28.6%)	2 (14.2%)[b]	4 (57.1%)	0.042[a]
Recurrence	13 (61.9%)	7 (50.0%)[b]	6 (85.7%)	0.112

[a] $p < 0.05$ was statistically significant.
[b] Two patients were not included due to one having a follow-up time of less than 1 year and one being lost to follow-up for 2 years.

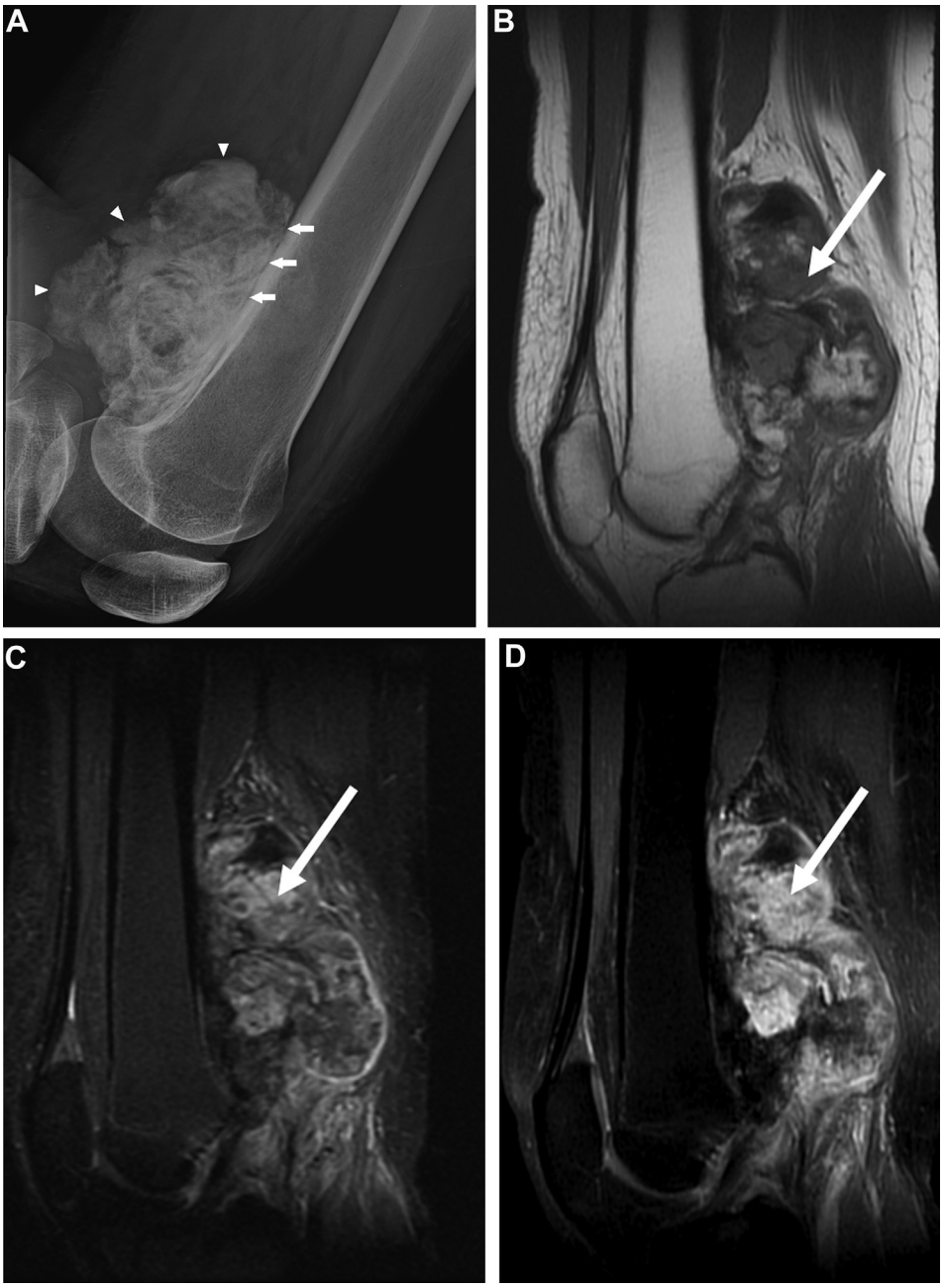

Fig. 1. A 33 year-old female exhibited low-grade parosteal OGS at the left distal femur. (**1A**) The lateral view of the radiography revealed classical ossified mass on the periosteum (arrowheads) with a presence of string sign, a radiolucent line separating the ossified mass and underlying cortex (arrows); MRI of the sagittal section of the mass revealed a heterogeneous signal, with the solid component predominately hypointense on T1-WI (arrow) (**1B**), hyperintense on T2-WI (arrow) (**1C**), and well enhancement on T1-WI with fat saturation after gadolinium contrast enhancement (arrow) (**1D**).

and one patient with lamellated periosteal reaction. We observed six cases of dedifferentiated parosteal OGS group with either type of periosteal reaction (85.7%), including four cases of sunburst periosteal reaction, and two cases of Codman triangle ($p = 0.266$). Interestingly, when sunburst periosteal reaction was analyzed independently, it was observed in two cases of the low-grade type (12.5%) and four cases of the dedifferentiated type (57.1%), respectively ($p = 0.025$), with a significantly higher incidence in dedifferentiated type (Fig. 2).

The imaging parameters of tumor necrosis, hemorrhage, soft tissue component, perforating vessels, average ossification grade, marginal ossification, bone marrow edema, bone marrow invasion, regional soft tissue edema, adjacent joint involvement, adjacent neurovascular bundle compression, regional lymph node enlargement, neighboring bone metastasis, and local recurrence all demonstrated no statistically significant difference between the low-grade group and dedifferentiated group ($p > 0.05$).

None of our studied cases in both groups revealed preoperative lung metastasis. However, lung metastasis was noted in two cases of the low-grade type (14.2%), and four cases of the dedifferentiated type (57.1%) in the follow-up imaging,

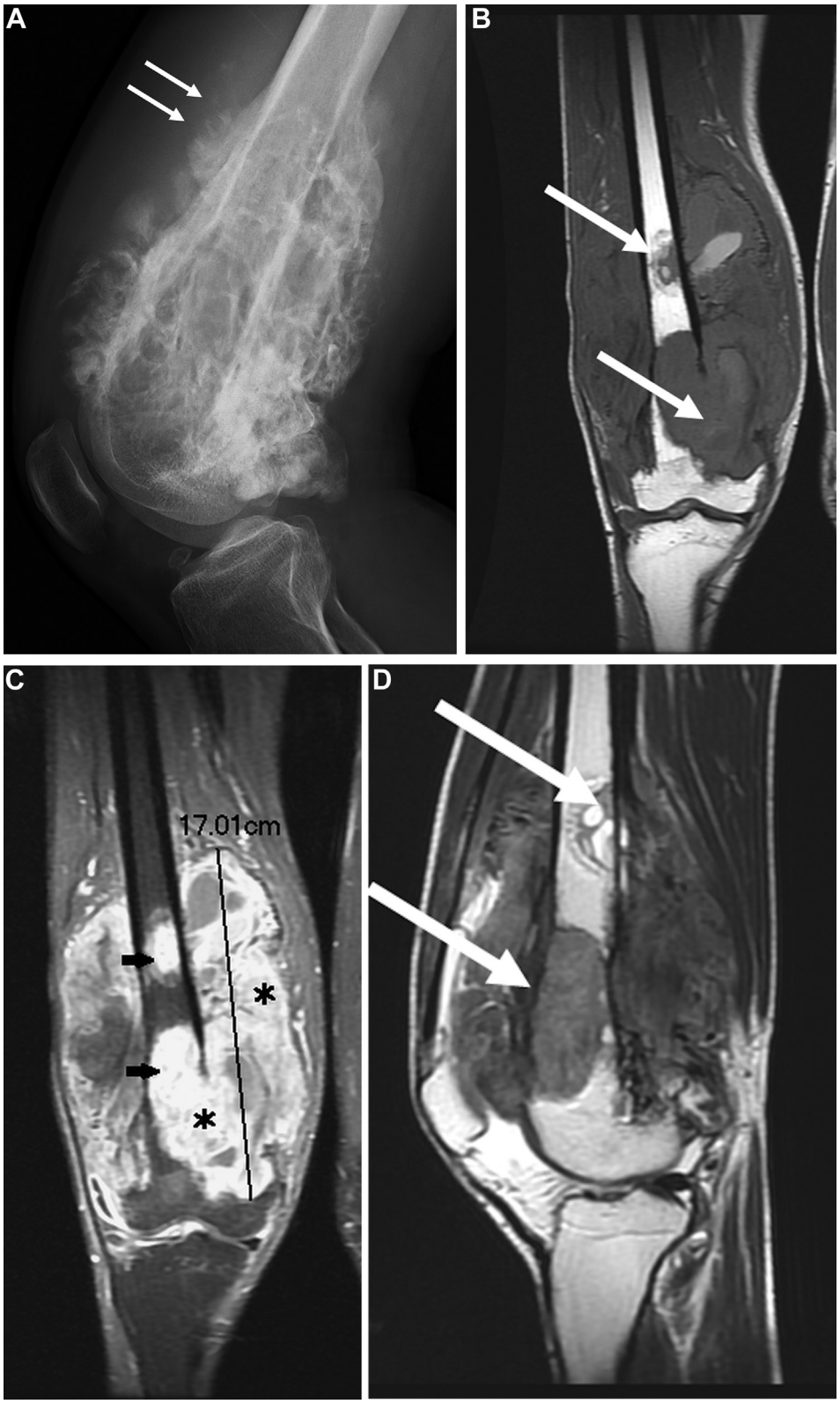

Fig. 2. A 32 year-old man with dedifferentiated parosteal OGS at right distal femur. Radiography of lateral view demonstrated a sunburst periosteal reaction (arrows) (2A); MRI of coronal section revealed a bulky mass over 17 cm in length, a solid tumor component (*), bone invasion (arrows) in T1-WI (2B) and the post-Gadolinium contrast enhancement of T1-WI with fat saturation (2C); Sagittal T2-WI revealed bone marrow invasion (arrows) (2D).

respectively ($p = 0.040$). Two patients were not included due to one having a follow-up time less than 1 year and one being lost to follow-up for 2 years.

In the ROC analysis, average tumor size, and sunburst periosteal reaction were revealed to exhibit the largest area under the curve (AUC = 0.70, 0.72, respectively) in the

differential diagnosis of dedifferentiated and low-grade parosteal OGS (Fig. 3). The cutoff value of the maximal tumor size for dedifferentiated type was 11 cm, with a sensitivity of 43% and a specificity of 87%. The sunburst periosteal reaction for the detection of dedifferentiated type exhibited a sensitivity of 57% and a specificity of 87%.

4. Discussion

The major finding of our study is that the imaging parameters of "tumor size with a cutoff value of 11 cm" and "sunburst periosteal reaction" demonstrated significant diagnostic value in distinguishing between low-grade parosteal OGS and dedifferentiated parosteal OGS. Both parameters indicated average sensitivity (43% and 57%, respectively), but high specificity (87% and 87%, respectively). If the tumor size is greater than 11 cm or the presence of sunburst periosteal reaction is observed, dedifferentiated parosteal OGS should be highly suspected.

Yarmish et al. reported that the size of the soft-tissue component is related to the differentiation or high-grade of parosteal OGS.[1] In our study, tumor length was one of the most important parameters. The average maximal tumor length in dedifferentiated parosteal OGS was 10.9 cm, longer than that of the low-grade parosteal OGS (7.1 cm). A similar finding was observed in a nationwide cohort study with a median length of 6 cm in low-grade and 11 cm in dedifferentiated parosteal OGS.[11] We assumed that dedifferentiated type parosteal OGS exhibits more aggressive tumor behavior, and therefore grows more rapidly compared with the low-grade type. Several studies have reported the characteristic chromosomal aberrations in low-grade parosteal OGS, the so-called "ring chromosomes" composed of 12q13-15 gains.[9,12] Yoshida et al. reported that MDM2 and CDK4 immunohistochemical coexpression occurred rarely in primary and recurrent/metastatic high-grade osteosarcomas, but that in tumors they demonstrated evidence of being transformed from precursor low-grade osteosarcomas.[13] However, the exact role of chromosome 12 alterations or other genetic expressions in the pathogenesis of dedifferentiated parosteal OGS, and the possible clinical association with tumor behavior and growth rate have not been reported in the literature, and require further investigation.

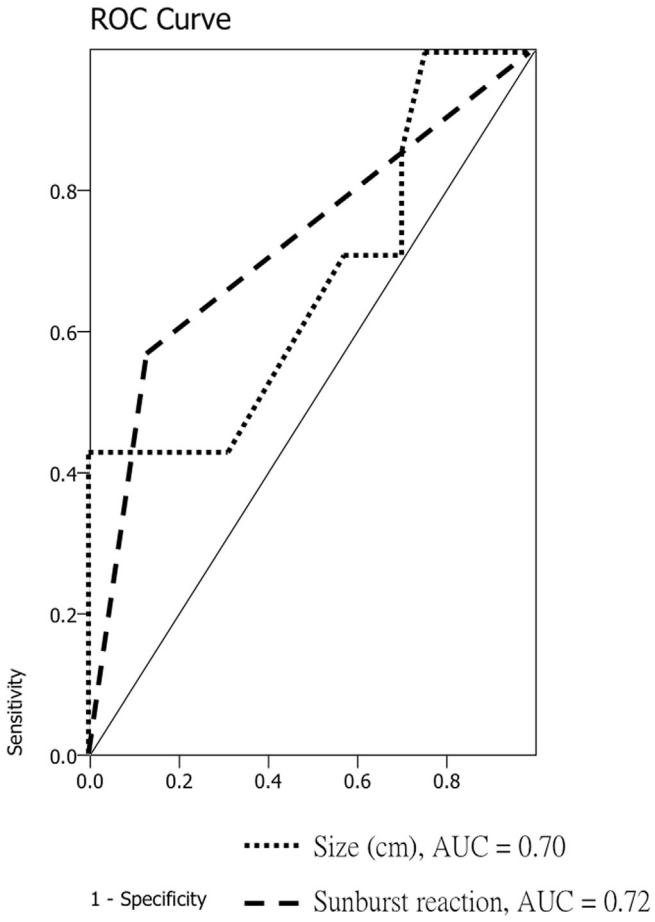

Fig. 3. In the receiver operating characteristic (ROC) curve analysis, the area under the curve (AUC) indicated that "size" and "sunburst periosteal reaction" are two clinically crucial imaging parameters in distinguishing between dedifferentiated parosteal OGS and low-grade parosteal OGS.

The periosteum is a thin membrane that covers most bone structures, and exhibits osteogenic activity. It is a dynamic structure that plays a major role in bone modeling and remodeling under normal conditions. In several disorders such as infections, benign and malignant tumors, and systemic diseases, the osteogenic potential of the periosteum is stimulated and new bone is produced, in a so-called periosteal reaction.[14] The periosteal reaction can be classified into six patterns: solid, single lamellar, multilamellar (onion–skin reaction), spiculated, peculiar (shell), and interrupted periosteal reactions.[14] A periosteal reaction was generally a sign of parosteal OGS in our case series. A valuable finding is that a sunburst periosteal reaction exhibits the characteristics of high-grade malignant potential in parosteal OGS. A sunburst periosteal reaction is frequently observed in conventional OGS, and less frequently in parosteal OGS. In dedifferentiated parosteal OGS, the sunburst periosteal reaction is more frequent compared with low-grade type parosteal OGS (57.1% vs 12.5%, $p = 0.025$). The sunburst periosteal reaction is a subtype of the spiculated periosteal reaction, with the appearance of divergent spicules perpendicular to the underlying cortex (Fig. 2). It combines a periosteal reaction and the production of osteoid in a malignant process, both being interrelated and difficult to differentiate by histopathological studies.[14] It usually occurs in conditions such as conventional osteosarcoma, metastasis (especially from the sigmoid colon and rectum), Ewing sarcoma, haemangioma, meningioma, tuberculosis, and tropical ulcers.[15] This pattern implies a faster growth and a more aggressive process than those of solid or lamellar periosteal reactions, and is usually malignant.[14] Therefore, our study demonstrated that dedifferentiated parosteal OGS, a more malignant and aggressive subtype of parosteal OGS, was characterized by a higher incidence of sunburst periosteal reaction.

Previous reports have revealed that the dedifferentiation of parosteal OGS correlates radiographically with increased lysis

or radiolucency in a highly mineralized area, hypervascularity, and the presence of a soft-tissue mass with ill-defined margins.[8,16,17] However, in our study overlaps existed in the distributions of tumor necrosis, hemorrhage, and solid soft tissue mass in dedifferentiated and low-grade parosteal OGS, without significant differences. Similar findings were reported in the study of Okada et al.[18] Tumor involvement of the medullary bone was approximately 22%–58%.[6,19–21] In the past, medullary involvement was thought to be an adverse outcome,[9] but most recent studies have indicated that it has no effects on histologic grading and survival.[9,22,23] We discovered that dedifferentiated parosteal OGS has a higher potency of bone marrow involvement (57.1%) compared with the low-grade type (37.5%), but without significant differences ($p = 0.332$).

The classical MRI of a major section of the parosteal OGS emits low signals on T1-and T2-WI due to massive ossification.[1] The soft-tissue component was observed in nearly all tumors, and peripheral ossification was more prominent than central ossification (in more than 50% of cases), which may mimic myositis ossificans. In our series, there was 34.8% marginal ossification in parosteal OGS.

The typical parosteal OGS has a string sign, perhaps up to 65%, with a cleavage plane along the cortex.[24] In our study, the string sign was observed in 8 out of 23 cases (34.8%), and no significant difference was discovered between the low-grade type and dedifferentiated type ($p = 0.591$).

Our study analyzed both preoperative lung metastasis and lung metastasis in the follow-up imaging. We want to provide early imaging clues to help distinguish between the two types of parosteal OGS before surgical resection, but none of our studied cases revealed definite lung metastasis before surgery. One of the patients in the low-grade group had several ground glass opacities in both lungs, and after consultation with a radiologist who specialized in chest imaging, the imaging pattern was more indicative of multifocal slow-growing lung cancer. Therefore, preoperative lung metastasis cannot be used as a predictive parameter to differentiate between the two types of parosteal OGS. However, the follow-up imaging revealed lung metastasis in two cases of the low-grade type (14.2%), and four cases of the dedifferentiated type (57.1%), respectively ($p = 0.040$). We can conclude that dedifferentiated parosteal OGS is more commonly to develop lung metastasis in the future.

The incidence of dedifferentiated parosteal OGS has been previously reported to account for up to 24%–43% of all parosteal OGSs, and the clinical pattern was considerably different from low-grade parosteal OGS.[9] Dedifferentiated parosteal OGS has a capability of developing increased distant metastasis, in which the pulmonary metastasis rate was approximately 25%–50%.[9,22,24] Our observation in dedifferentiated parosteal OGS also revealed a 57.1% lung metastasis in the follow-up studies compared with 14.2% in the low-grade type. In addition, the mortality rate of dedifferentiated parosteal OGS could reach 28%–50%.[9,25] Due to the poor outcome related to conventional high-grade OGS, neoadjuvant chemotherapy (chemotherapy before surgery) was suggested to improve the survival.[11,22] On the contrary, with low-grade parosteal OGS, the safe margin for dedifferentiated parosteal OGS resection cannot be compromised due to the high malignancy. Thus, to decide on both the use of neoadjuvant chemotherapy and surgical margin, precisely distinguishing low-grade or dedifferentiated parosteal OGS before surgery is crucial. According to our study results, in clinical practice, if the preoperative imaging evaluation reveals a tumor size greater than 11 cm or the presence of a sunburst periosteal reaction, dedifferentiated parosteal OGS should be highly suspected instead of low-grade parosteal OGS. The limited sensitivity may result from the limited number of cases, and further data collection and observation may be necessary.

We acknowledge the limitations of this study. First, this is a retrospective study. The imaging evaluation was performed with established protocols in our hospital. We did not perform a dynamic contrast study, and this may provide us with more information for distinguishing the two types of parosteal OGS. Furthermore, we evaluated tumor size at the initial imaging, but we could not evaluate the growth rate or doubling time of the tumor. We suggest that future prospective studies should focus on different imaging protocols, different imaging modalities, and tumor growth rates. Second, the number of cases was limited. However, the parosteal OGS is a rare type of OGS, and thus a study of 23 cases of parosteal OGS still could afford researchers and medical practitioners with a valuable point of reference.

In conclusion, imaging studies revealed crucial value in differentiating low-grade parosteal OGS and dedifferentiated parosteal OGS. Compared with low-grade parosteal OGS, the dedifferentiated type revealed significantly larger in tumor size and more sunburst periosteal reaction, and both factors revealed good specificity.

References

1. Yarmish G, Klein MJ, Landa J, Lefkowitz RA, Hwang S. Imaging characteristics of primary osteosarcoma: nonconventional subtypes. *Radiographics* 2010;**30**:1653–72.
2. A review of the WHO classification of tumours of soft tissue and bone. Website. http://sarcomahelp.org/reviews/who-classification-sarcomas.html Published 2013. Accessed December 25, 2017.
3. Wu PK, Chen WM, Chen CF, Lee OK, Haung CK, Chen TH. Primary osteogenic sarcoma with pulmonary metastasis: clinical results and prognostic factors in 91 patients. *Jpn J Clin Oncol* 2009;**39**:514–22.
4. Hung GY, Yen HJ, Yen CC, Wu PK, Chen CF, Chen PC, et al. Improvement in high-grade osteosarcoma survival: results from 202 patients treated at a single institution in Taiwan. *Medicine (Baltim)* 2016;**95**:e3420.
5. Hung GY, Yen HJ, Yen CC, Chen WM, Chen PC, Wu HT, et al. Experience of pediatric osteosarcoma of the extremity at a single institution in Taiwan: prognostic factors and impact on survival. *Ann Surg Oncol* 2015;**22**:1080–7.
6. Encinas-Ullán CA, Ortiz-Cruz EJ, Barrientos-Ruiz I, Valencia-Mora M, González-López JM. Parosteal osteosarcomas: unusual findings. *Rev Esp Cir Ortop Traumatol* 2012;**56**:281–5.
7. Shah A, Ma H, Sun X, Cao D. Primary parosteal osteosarcoma of the rib. *Interact Cardiovasc Thorac Surg* 2012;**15**:169–70.
8. Hang JF, Chen HPC. Parosteal osteosarcoma. *Arch Pathol Lab Med* 2014;**138**:694–9.

9. Bertoni F, Bacchini P, Staals EL, Davidovitz P. Dedifferentiated parosteal osteosarcoma: the experience of the Rizzoli Institute. *Cancer* 2005;**103**:2373−82.
10. Sheth DS, Yasko AW, Raymond AK, Ayala AG, Carrasco CH, Benjamin RS, et al. Conventional and dedifferentiated parosteal osteosarcoma. Diagnosis, treatment, and outcome. *Cancer* 1996;**78**:2136−45.
11. Okada K, Unni KK, Swee RG, Sim FH. High grade surface osteosarcoma: a clinicopathologic study of 46 cases. *Cancer* 1999;**85**:1044−54.
12. Gamberi G, Ragazzini P, Benassi MS, Ferrari C, Sollazzo MR. Analysis of 12q13-15 genes in parosteal osteosarcoma. *Clin Orthop Relat Res* 2000:195−204.
13. Yoshida A, Ushiku T, Motoi T, Beppu Y, Fukayama M, Tsuda H, et al. MDM2 and CDK4 immunohistochemical coexpression in high-grade osteosarcoma: correlation with a dedifferentiated subtype. *Am J Surg Pathol* 2012;**36**:423−31.
14. Bisseret D, Kaci R, Lafage-Proust MH. Periosteum: characteristic imaging findings with emphasis on radiologic-pathologic comparisons. *Skeletal Radiol* 2015;**44**:321.
15. Mohammadi A, Ilkhanizadeh B, Ghasemi-Rad M. Mandibular plasmocytoma with sun-ray periosteal reaction: a unique presentation. *Int J Surg Case Rep* 2012;**3**:296−8.
16. Berner K, Johannesen TBXR, Bruland XYS. Clinical epidemiology of low-grade and dedifferentiated osteosarcoma in Norway during 1975 and 2009. *Sarcoma* 2015:1−9.
17. Jelinek JS, Murphey MD, Kransdorf MJ, Shmookler BM, Malawer MM, Hur RC. Parosteal osteosarcoma: value of MR imaging and CT in the prediction of histologic grade. *Radiology* 1996;**201**:837−42.
18. Okada K, Frassica FJ, Sim FH, Beabout JW, Bond JR, Unni KK. Parosteal osteosarcoma: a clinicopathological study. *J Bone Joint Surg Am* 1994;**76**:366−78.
19. Campanacci M, Picci P, Gherlinzoni F, Guerra A, Bertoni F, Neff JR. Parosteal osteosarcoma. *J Bone Joint Surg Br* 1984;**66**:313−21.
20. Unni KK, Dahlin DC, Beabout JW, Ivins JC. Parosteal osteogenic sarcoma. *Cancer* 1976;**37**:2466−75.
21. Abdelwahab IF, Kenan S, Hermann G, Klein MJ. Dedifferentiated parosteal osteosarcoma of the radius. *Skeletal Radiol* 1997;**26**:242−5.
22. Cardona DM, Knapik JA, Reith JD. Dedifferentiated parosteal osteosarcoma with giant cell tumor component. *Skeletal Radiol* 2008;**37**:367−71.
23. Futani H, Okayama A, Maruo S, Kinoshita G, Ishikura R. The role of imaging modalities in the diagnosis of primary dedifferentiated parosteal osteosarcoma. *J Orthop Sci* 2001;**6**:290−4.
24. Laitinen M, Parry M, Albergo JI, Jeys L, Abudu A, Carter S, et al. The prognostic and therapeutic factors which influence the oncological outcome of parosteal osteosarcoma. *Bone Joint Lett J* 2015;**97-B**:1698−703.
25. Partovi S, Logan PM, Janzen DL, O'Connell JX, Connell DG. Low-grade parosteal osteosaracoma of the ulna with dedifferentiation into high-grade osteosarcoma. *Skeletal Radiol* 1996;**25**:497−500.